HHS Public Access

Author manuscript

J Alzheimers Dis. Author manuscript; available in PMC 2018 January 31.

Published in final edited form as:

J Alzheimers Dis. 2017 ; 59(2): 575–590. doi:10.3233/JAD-170173.

Overexpression of ubiquilin-1 alleviates Alzheimer's disease-caused cognitive and motor deficits and reduces amyloid-β accumulation in mice

Oludotun O. Adegoke[§], **Fangfang Qiao**[§], **Yanying Liu**, **Kirsty Longley**, **Shelley Feng**, and **Hongmin Wang**[*]

Division of Basic Biomedical Sciences and Center for Brain and Behavior Research, University of South Dakota Sanford School of Medicine, Vermillion, SD 57069, USA

Abstract

Ubiquilin-1 (Ubqln1) is a ubiquitin-like protein that has been implicated in Alzheimer's disease (AD). However, whether Ubqln1 modulates learning and memory and alters AD-like behavior and/or pathology have not been determined in animal models. To understand the function of Ubqln1 *in vivo*, we previously generated Ubqln1 transgenic (TG) mice that overexpress mouse Ubqln1. With the model, we here characterized the TG mouse cognitive behaviors and found that Ubqln1 TG mice showed better spatial learning and memory capabilities than their wild-type littermates in both radial arm water maze and Y-maze tests. Additionally, we crossed the Ubqln1 TG mice with the AβPPswe/PSEN1dE9 double transgenic AD mouse to generate the AD/Ubqln1 triple TG (AD/TG) mice. Our results suggest that at 12 months of age following the onset of AD, AD/TG mice showed better spatial learning and memory than AD mice. AD/TG mice also exhibited better motor function than AD mice at the same age. Furthermore, compared to AD mice, AD/TG mice showed significant reduction in amyloid-β 40 ($A\beta_{40}$) and $A\beta_{42}$ levels in the cerebral cortex and in the hippocampus at the post-onset stage. The number of Aβ plaques was significantly decreased in the cerebral cortex of AD/TG mice at this post-onset stage. Moreover, mature AβPP level in AD/TG hippocampus was lower than that in AD hippocampus. These data not only provide a direct link between overexpression of Ubqln1 and altered learning and memory but also raise the possibility that Ubqln1 is a potential therapeutic target for treating AD and possibly other neurodegenerative disorders.

Keywords

Ubiquilin-1; Alzheimer's disease; learning and memory; amyloid-β; plaques

[*]Correspondence author: Hongmin Wang, Division of Basic Biomedical Sciences, Sanford School of Medicine, University of South Dakota, Vermillion, SD 57069, USA, Telephone: 605-658-6382, Fax: 605-677-6381, Hongmin.Wang@usd.edu.

[§]These authors contributed equally to the work.

COMPETING INTEREST DISCLOSURE

The authors declare no competing financial interests.

INTRODUCTION

Alzheimer's disease (AD), a neurodegenerative disorder, is characterized by progressive memory loss (dementia) and impairment of cognitive function. AD is the leading cause of dementia and accounts for 60 to 80 percent cases of dementia in the elderly [1]. The cause for most AD cases remains largely unknown [2] except for a small fraction of cases where mutations in amyloid-β precursor protein (AβPP), the presenilin-1 (PSEN1) and presenilin-2 (PSEN2) cause the early-onset familial form of AD and increase the level of amyloid- β (Aβ) peptides [3]. AβPP is a transmembrane protein that can be cleaved to release Aβ peptides through sequential proteolytic processing carried out by β- and γ-secretases [4]. The γ-secretase is an enzyme complex consisting of PSEN, PSEN enhancer 2 (PEN-2), anterior pharynx-defective 1, and nicastrin [5]. β-secretase cleavage of AβPP results in the release of AβPP ectodomain, leaving the AβPP C-terminal fragment within the membrane. Subsequently, this is followed by the γ-secretase cleavage that produces the Aβ peptides. To study AD, many transgenic mice have been generated to overexpress one or multiple familial AD mutations to model the disorder. One well characterized AD transgenic mouse model is the AβPPswe/PSEN1dE9 mouse that bears both a mutated AβPP and a mutated PSEN1 and shows amyloid pathology in the brain as early as 4 months and deficits in cognitive function at 6 months [6].

Ubiquilin-1 (Ubqln1, also known as PLIC-1) is a ubiquitin-like protein that contains an N-terminal ubiquitin-like domain which mediates interaction with the proteasome and a C-terminal ubiquitin-associated domain that binds to poly-ubiquitinated proteins. Unlike those small ubiquitin-like proteins, such as SUMO [7] and NEDD8 [8–10], Ubqln1 cannot be covalently conjugated to target proteins. It is considered to function as an ubiquitin shuttle factor/adaptor protein to mediate protein degradation via the ubiquitin proteasome system (UPS) and also possibly autophagy [11–13] and to reduce oxidative stress-induced neurotoxicity [14]. Several lines of studies have linked Ubqln1 to AD. First, Ubqln1 interacts with PSEN, one of the major γ-secretase components, and regulates protein degradation [15, 16] as well as γ-secretase activity [17]. Second, Ubqln1 regulates AβPP maturation and degradation [18]. Third, Ubqln1 modulates AβPP trafficking, processing, and Aβ secretion in culture cells [19]. Fourth, Ubqln1 is associated with neurofibrillary tangle pathology [20] and its protein levels are reduced in AD patient brains [21, 22], which may contribute to increased Aβ production. Finally, single nucleotide polymorphisms in the Ubqln1 gene may be associated with AD [23–25]. Although these observations have shed great light on our understanding of the possible role of Ubqln1, the relation between Ubqln1 and learning and memory and whether Ubqln1 modulates AD pathogenesis have not been determined. To better understand biological function of Ubqln1 *in vivo*, we previously generated Ubqln1 transgenic (TG) mice globally overexpressing Ubqln1 in multiple tissues including brain [14]. With this mouse, we here examined spatial learning and memory behaviors of TG mice and compared with their wild-type (Wt) littermates. Additionally, we also crossed the Ubqln1 TG mice with the AβPPswe/PSEN1dE9 AD double transgenic mouse model to generate the Ubqln1/AD triple TG (AD/TG) mice and then compared their cognitive and motor behaviors and neuropathology with their AD littermates.

MATERIALS AND METHODS

Animals

Generation of Ubqln1 TG mice was previously described [14]. The Ubqln1 TG mice were then repeatedly crossed with C57BL/C3H mice to generate a sizeable amount of Ubqln1 TG mice and Wt littermates used in this study. The AβPPswe/PS1dE9 AD mice (in the C57BL background) were obtained from Jackson Laboratory (Bar Harbor, Maine, USA) and were crossed with Ubqln1 mice (in the C57BL/C3H hybrid background) to generate AD and AD/Ubqln1-TG triple transgenic (AD/TG) mice. AD and AD/TG-positive mice were identified by PCR using the primers as described previously [14, 26]. All mice were handled according to procedures that were approved by the Institutional Animal Care and Use Committee of the University of South Dakota. Mice were maintained at room temperature with a regular light/dark cycle of 12/12 hours (h). Mice were allowed to access food and water *ad libitum*. All behavioral tests were performed during the light phase of the circadian cycle.

Based on their genotypes and ages, mice between 4 to 5 months were classified as pre-onset group, either pre-onset AD or pre-onset AD/TG group, while mice at 12 months were classified as post-onset group, either post-onset AD group or post-onset AD/TG group. The pre-onset group represents the period of onset of deposition of amyloid plaques in the brain with little or no cognitive deficits [26], while the post-onset group represents the period when the cognitive defects following amyloid plaque deposition are much manifest [27].

Radial arm water maze (RAWM) test

The RAWM test was used to evaluate spatial learning and memory. It involves a 2-day protocol that has been previously described [28–30]. Briefly, RAWM consisted of a circular pool of 0.96 m diameter and 23.8 cm deep with six swim arms that was each 28 cm wide and 30 cm long radiating out from an open central area (38 cm in diameter). Four spatial cues were present at each of four quadrants around the testing room but not in the maze. An escape platform was located at the end of one arm (the goal arm) and the goal arm remained constant for all trials of each mouse. On each trial, the mouse was started in one arm that did not contain the platform and allowed to swim for 60 seconds (s) to find the escape platform. The start arm was varied on successive trials. Furthermore, the goal arm was placed in a different location for subsequent mice to exclude any odor cue. If the mouse was not able to locate the platform after 60 s, the mouse was gently guided to the platform. The mouse was allowed to stay on the platform for 15 s, no matter it was guided or located the platform within 60 s. On day 1, each mouse was trained for 15 trials and each trial alternated between visible and hidden platform in the goal arm with the goal arm constant for each mouse. On day 2, each mouse was trained for 15 trials with the hidden platforms only. Entry into an arm was defined as all four paws within one radial arm and body parallel to the alley wall. Each entry into an incorrect arm not containing the escape platform or failing to select an arm after 15 s was scored as an error. Each consecutive 3 trials were averaged to give a block. Thus, there were 5 blocks on each day. Experimenters were blinded to the genotypes of the mice at the time of testing.

Y-maze test

The Y-maze apparatus was also used to evaluate learning and memory with more emphasis on working and short term memory. It consisted of three equilateral arms made of transparent polystyrene (30 cm × 8 cm × 20 cm) and was mounted on a white base. The inside of the arms was identical. There were no platforms and no internal cue provided. The maze was placed in a well-lit room containing a variety of external cues. The floor of the Y-maze was covered with a thin (0.5 cm) layer of wood chip bedding material and redistributed between trials to prevent use of odor cues. To make the olfactory environment more similar for the first versus following mice, two non-experimental mice were placed in the maze for a few minutes before each trial starts; after which the bedding materials were reshuffled.

Each mouse was placed in an arm of the Y-maze (start arm), one of the arms was blocked with an opaque door (novel arm). The mouse was allowed to explore the start arm and remaining arm (other arm) for 5 min (training phase). The mouse was then removed and returned to its home cage, the novel arm was then unblocked and the bedding mixed. After 1 hour (h) delay, the mouse was placed into the start arm and allowed to explore all three arms freely for 2 minutes (test phase). The number of arm entries and time spent in each arm was recorded by the experimenter who was blinded to the genotype of the mice. An entry into an arm was defined by a mouse placing all four paws inside an arm.

Rotarod test

This test was used to evaluate mouse motor coordination and strength and was conducted using an accelerating rotarod machine (Med Associates Inc., St Albans, VT, USA). The cylinder rotated at an initial rate of 3.5 rotations per minute (rpm) and accelerated gradually to 20–40 rpm. When a mouse could no longer stay on the rod, it fell and the amount of time that the mouse remained on the accelerating rod was recorded. The cut-off duration of each trial was 250 s and the average for three trials was evaluated. Before the formal test, each mouse underwent training of three trials each day for three days before the test day.

String agility test

This test was used to test agility and grip capacity. The protocol was described in a previous study [31]. Each mouse was allowed to grasp a suspended string only using their forepaws and subsequently released by the experimenter. The maximum trial length was 60 s. The scoring system to assess the grasp capacity involved a five scale system: 0-unable to remain on string; 1-hangs by two forepaws; 2-attempts to climb to string; 3-hangs by two forepaws and one or two hind paws around string; 4-four paws and tail around string; 5-escape.

The sequence of behavioral experiments involved performing experiments with less aversive stimuli earlier and experiments with more aversive experiments done later. It should be noted that only one type of behavioral experiment was performed per day allowing for a minimum of 24 h rest before subsequent experiments were performed. The sequence of behavioral experiments was as follows: string agility test, rotarod test, Y-maze test, and RAWM test.

Enzyme-linked immunosorbent assay (ELISA)

Soluble $A\beta_{40}$ and $A\beta_{42}$ were quantified in the cerebral cortex and hippocampus from mice in the pre-onset and post-onset groups using human $A\beta_{40}$ and $A\beta_{42}$ ELISA kits (ThermoFisher Scientific, Waltham, MA, USA) according to the manufacturer's instructions. Absorbance was measured with the BioTek ELx808 Absorbance Microplate Reader (BioTek, Winooski, VT, USA) and data was expressed as pg/ml.

Histopathological analysis

Mice were perfused with phosphate-buffered saline and brains were fixed in 4% paraformaldehyde for at least 48 h. Subsequently, they were transferred to 40% sucrose and allowed to slowly spin for about 72 h at 4°C until the brain samples settled at the bottom of a tube. The brain samples were cryo-frozen with OCT mounting medium (Tissue-Tek, Sakura Finetek, USA) and then the coronal sections of the cerebral cortex were cut at 40 μm thickness. The sections were then stained with Thioflavin S as described in a previous study [32]. Briefly, brain sections were incubated consecutively in 70% Ethanol, 80% Ethanol, and 0.1% Thioflavin S solution. The stained sections were then consecutively washed with 80% Ethanol, 70% Ethanol, and distilled water before mounting in aqueous media. The stained sections were analyzed using a Zeiss Upright M-1 fluorescent microscope under 5× magnification with a green fluorescence channel. Quantification of amyloid plaques was performed using the FIJI software. Four coronal sections showing the cerebral cortex were analyzed for each mouse and the average number of plaques was calculated. The number of amyloid plaques in each slide was counted with the pointer tool of the software and recorded.

Immunoprecipitation, Western blot and protein band quantitation

To detect ubiquitinated AβPP, mouse brain cortical tissues were homogenized on ice with a Dounce homogenizer in IP buffer (0.5% NP-40, 500 mM Tris–HCl, pH 7.4, 20 mM EDTA, 10 mM NaF, 30 mM sodium pyrophosphate decahydrate, 2 mM benzamidine, 1 mM phenylmethanesulfonylfluoride, 1 mM N-ethyl-maleimide and a cocktail of protease inhibitors). The lysates were then incubated on ice for 30 min before being centrifuged for 5 min at 2000 × g. The supernatants were incubated with protein A/G-coupled beads (EMD Millipore, Billerica, MA, USA) and 5 mg of the anti-AβPP C-terminal antibody (Sigma, St Louis, MO, USA) at 4°C for 2 h. After washing the beads with IP buffer, proteins were eluated, separated on a SDSPAGE gel (ThermosFisher), transferred onto a nitrocellulose membrane, and probed with an anti-ubiquitin (Cell Signaling, Danvers, MA, USA) and anti-AβPP antibodies (Sigma). Appropriate secondary antibodies conjugated with fluorescent dyes (LI-COR Inc., Lincoln, NE, USA) were used.

For Western blot analysis of Ubqln1 and AβPP, mouse brain cortex or hippocampus was lysed in a protein extraction buffer [33], separated by SDS-PAGE, transferred onto a nitrocellulose membrane, and probed with an anti-Ubqln1 (Abcam), anti-AβPP (Cell Signaling), anti-actin, and/or anti-GAPDH antibodies (Santa Cruz Biotechnology). Appropriate secondary antibodies conjugated with fluorescent dyes (LI-COR Inc.) were used.

For Western blot analysis of immature and mature AβPP and C99 and C83 fragments of the protein, we followed a previously described method [17]. Briefly, mouse brain cortex or hippocampus was homogenized in an appropriate volume of tissue protein extraction buffer (ThermoFisher) supplemented with EDTA-free protease inhibitor cocktail (Sigma). The protein lysates were then centrifuged at 10,000 × g for 10 min at 4 °C. Protein concentrations were measured with the NanoDrop (ThermoFisher). Proteins (30 μg) were separated on 4 to 12% Bis-Tris gels (ThermoFisher) under denaturating conditions and transferred onto polyvinylidene difluoride (PVDF) membranes (GE Healthcare). The PVDF membrane was then immunoprobed with an anti-AβPP C-terminus (Sigma) and an anti-ubiquitin (Cell Signaling) antibodies.

To quantitate protein band intensities, protein bands were detected using an Odyssey scanner (LI-COR) and quantified using UN-SCAN-IT gel6.1 software (Silk Scientific Inc., Orem, Utah, USA).

Statistical analysis

All numerical data were presented as mean ± SEM or mean ± SD. For the RAWM test, the average errors to find the platform were calculated in blocks of consecutive 3 trials. A repeated measure two-way ANOVA followed by Holm-Sidak post-hoc test was used for comparisons between different genotypes at each block. A repeated measure one-way ANOVA followed by Tukey post-hoc test was used for behavioral comparisons between different time points (blocks) within each genotype to test for learning/memory over time in that genotype. For the rotarod test, a repeated measure two-way ANOVA followed by Holm-Sidak post-hoc test was used for comparisons between different genotypes on each day; while a one-way ANOVA followed by a student's t-test was used for comparisons between different ages within each genotype. For Y-maze test and all other experiments, data analysis was done by one-way ANOVA followed by a student's t-test. Significance was accepted as $p < 0.05$. Microsoft Excel 2013 and GraphPad Prism Statistical Software version 7.0 were used for statistical analysis and graphical display.

RESULTS

Ubqln1 TG mice show enhanced learning and memory compared to Wt littermates

To investigate whether Ubqln1 plays a role in learning and memory, we generated Ubqln1 transgenic (TG) mice which showed apparent overexpression of Ubqln1 in different tissues [14]. Since the RAWM test is a sensitive method for assessing small animals' learning and memory capability [28, 34], we therefore applied this method to compare the spatial learning and memory in Wt and TG mice at 2 months of age. As shown in Fig. 1A, the TG mice showed significantly fewer errors in finding the platform compared to their Wt littermates, specifically in block 8 and 10 on day 2 (Fig. 1A). To confirm these observations, we performed the RAWM test using different cohorts of Wt and TG mice at 3 months of age. The results showed that the TG mice consistently showed fewer errors than the Wt mice (Fig. 1B). Additionally, we also employed a Y-maze test which is based on mouse innate curiosity to explore novel areas to further compare the spatial learning and memory capabilities between the Wt and TG mice. At 4.5 months of age, both Wt and TG mice made

similar numbers of total entries during maze exploration (Fig. 1C, right panel). However, TG mice entered the novel arm (arm entry) significantly more than the start and other arms after 1 h delay (Fig. 1C, left panel). These data suggest that overexpression of Ubqln1 enhances learning and memory in mice.

Overexpression of Ubqln1 alleviates spatial learning and memory deficits in AD mice

We next examined whether overexpression of Ubqln1 could ameliorate the cognitive deficiency in AD mice. To test this, Ubqln1 TG mice were crossbred with the AβPPswe/PSEN1dE9 double transgenic AD mouse to generate AD/Ubqln1 triple transgenic (AD/TG) mice. To evaluate cognitive capability, the RAWM test was performed in the four groups of mice, notably pre-onset AD, pre-onset AD/TG, post-onset AD, and post-onset AD/TG groups. In the pre-onset group (between 4 and 5 months of age), there were no differences in terms of errors between the AD and their AD/TG counterparts at any of the blocks (Fig. 2A). In the post-onset group (12 months of age), however, compared with AD counterparts, AD/TG mice displayed differences in block 3 on day 1 and blocks 6 and 7 on day 2 by making few errors in finding the hidden platform (Fig. 2B). Furthermore, we observed that pre-onset AD mice generally outperformed post-onset AD mice in RAWM test on both day 1 and day 2 at blocks 4 and 6 respectively, demonstrating that spatial learning and memory deficits worsened with age in the AD mouse model (Fig. 2C). Additionally, there were no differences in errors made between pre-onset AD/TG and post-onset AD/TG groups of mice at any individual block (Fig. 2D), indicating no worsening with age in AD/TG mice. We also observed that the pre-onset AD mice made few errors by the end of day 1 and day 2 (Fig. 2E). Few errors were also observed at the end of day 1 and overall by the end of day 2 in the pre-onset AD/TG group (Fig. 2F), suggesting that both genotypes at the pre-onset stage demonstrated spatial learning and memory capabilities. However, there were no significantly few errors in the post-onset AD group at the end of either day 1 or day 2, indicating spatial learning and memory deficits occurred at this state in the group of mice (Fig. 2G). The post-onset AD/TG demonstrated some degree of spatial learning deficits as they did not make few errors by the end of day 1; but overall they made few errors at the end of the experiment by day 2 (Fig. 2H). Taken together, these data suggest that Ubqln1 overexpression consistently alleviates the impaired learning and memory capability in AD mice as the disease progresses.

Overexpression of Ubqln1 improves motor function in AD mice

An early study has reported that the AβPPswe/PSEN1dE9 mice showed impaired sensorimotor gaiting with the progression of the disease [26]. Thus, we next assessed whether overexpression of Ubqln1 would improve motor function in AD mice by running a battery of behavioral test. Rotarod test was conducted to evaluate animal motor functions and coordination capabilities. At the pre-onset stage, AD/TG showed no difference in motor coordination when compared to their AD littermates (Fig. 3A). At the post-onset stage, however, the AD/TG mice showed improved motor co-ordination and strength than their AD littermates (Fig. 3B). We also noticed that the post-onset AD group of mice showed worsening of motor co-ordination in comparison to their pre-onset AD group, whereas there was no worsening of the motor co-ordination in the AD/TG group with age (Fig. 3C). To further test agility and forepaw strength, the string agility test was performed in the different

groups. At the pre-onset stage, there was no difference in strength between AD and AD/TG mice; however, at the post-onset stage, AD/TG mice showed significant higher agility and forepaw strength than the AD mice (Fig. 4A). Additionally, the post-onset AD showed worsening of agility and forepaw strength when compared to the pre-onset AD, while there was no difference in terms of agility and forepaw strength between the pre- and post-onset AD/TG group (Fig. 4B). These results indicate that motor co-ordination and forepaw strength worsen with the progression of the disease and that overexpression of Ubqln1 is likely beneficial to motor function in AD mice.

Overexpression of Ubqln1 decreases the levels of $A\beta_{42}$ and $A\beta_{40}$ in the brains of AD mice

To examine whether the improved learning and memory in AD/TG mice is correlated with the reduced $A\beta_{42}$ level in mouse brain, we sacrificed the mice following behavioral tests and measured the $A\beta_{42}$ levels in both cerebral cortex and hippocampus of both AD and AD/TG mice in the pre- and post-onset groups by ELISA. In the cerebral cortex, there were significant reduction of $A\beta_{42}$ levels in AD/TG mice compared with AD counterpart mice in both the pre- and post-onset groups (Fig. 5A). In the hippocampus, AD/TG mice displayed lower levels of $A\beta_{42}$ at pre- and post-onset stages when compared to AD mice counterparts (Fig. 5C). In addition, the $A\beta_{42}$ level dramatically increased with the progression of disease in both cerebral cortex and hippocampus of the two groups of mice (Figs. 5B & 5D). Similarly, AD/TG mice also showed lower levels of $A\beta_{40}$ in both the cortex (Fig. 5E) and hippocampus (Fig. 5G) in both groups compared to AD mice. Similar to $A\beta_{42}$, $A\beta_{40}$ level also showed remarkable increases with the progression of disease in both cerebral cortex and hippocampus of the two groups of mice (Figs. 5F & 5H). These results imply that overexpression of Ubqln1 reduces the levels of $A\beta_{42}$ and $A\beta_{40}$ in the AD mouse brains.

Overexpression of Ubqln1 reduces amyloid plaque burden in the brains of AD mice

To further investigate whether overexpression of Ubqln1 could alleviate the amyloid plaques, one of the key pathological characteristics of AD, we detected the number of amyloid plaque in the cerebral cortex in both AD and AD/TG mice at the pre- and post-onset stages using Thioflavin S staining. At both pre- and post-onset stages, age-related accumulation of amyloid plaques was identified in both AD and AD/TG groups (Fig. 6A). Quantification of amyloid plaques in the cerebral cortex showed significant decline in the burden of amyloid plaques in AD/TG mice compared to AD mice in both the pre- and post-onset stages (Fig. 6B). Furthermore, we observed a consistent increase in the amount of amyloid plaques with age in both groups (Fig. 6C). These data are consistent with the results of ELISA measurement of $A\beta_{42}$ level. These results suggest that overexpression of Ubqln1 positively diminished the amyloid plaque load, which may contribute to the better learning and memory observed in AD/TG mice.

Overexpression of Ubqln1 reduces mature AβPP level in the hippocampus of post-onset AD mice

We then examined whether the reduced $A\beta_{40}$, $A\beta_{42}$, as well as amyloid plaque burden altered mature AβPP level and AβPP processing in the cortex and hippocampus. Overexpression of Ubqln1 in the cortex and hippocampus of AD/TG mice were confirmed by western blot analysis of Ubqln1 protein levels (Figs. 7A & 7B, 7D & 7E, respectively).

Overexpression of Ubqln1 reduced mature AβPP level in the hippocampus (Figs. 7D & 7F) but not in the cortex (Figs. 7A & 7C) of the mice. However, overexpression of Ubqln1 appeared not to alter the levels of the two AβPP carboxyl-terminal fragments, C83 and C99 either in the cortex (Figs. 7A & 7C) or hippocampus (Figs. 7D & 7F). Thus, overexpression of Ubqln1 alleviates mature AβPP level but may not affect AβPP processing in the cortex and hippocampus of AD mice.

Overexpression of Ubqln1 does not affect AβPP ubiquitination level in post-onset AD mice

Previous data suggest Ubqln1 involves UPS-mediated protein degradation [11, 35]. To further define whether reduced AβPP maturation was associated with altered ubiquitination level of AβPP, we performed immunoprecipitation of AβPP using a carboxyl-terminal anti-AβPP antibody and then examined ubiquitinated AβPP level. As shown in Figs. 8A, 8B & 8C, ubiquitinated AβPP level in the AD/TG mouse cortex did not significantly differ from that in the AD mouse cortex, suggesting that overexpression of Ubqln1 may not affect AβPP ubiquitination in the brain region of AD mice.

DISCUSSION

Our results provide strong evidence showing that Ubqln1 plays a crucial role in modulating learning and memory function in different cohorts of transgenic mice as well as in the AD mice. When Ubqln1 is overexpressed, we observed improved spatial learning and memory in the adult mice at the post-onset stages AD. In accordance with the cognitive phenotype exhibited by the TG mice, overexpression of Ubqln1 in AD mice (AD/TG mice) also showed improved cognitive functions and reduced $A\beta_{42}$ levels and amyloid plaques, suggesting that Ubqln1 positively regulates spatial learning and memory.

The AβPPswe/PSEN1dE9 AD mouse model with both AβPPswe and PSEN1 mutations shows the amyloid plaque pathology as early as 4–6 months [26]. This allows for adequate study of both Aβ deposition and cognitive defects over a moderate period of time. Using this AD mouse model carrying mutations in both AβPP and PSEN1 as a baseline for AD, we were able to cross it with a transgenic mouse model that globally overexpressed Ubqln1 to generate AD/TG triple transgenic mice in which the effect of Ubqln1 in an AD mouse model could be studied. Previous results have shown notable behavioral differences between the AβPPswe/PSEN1dE9 AD mice and the non-transgenic wild-type mice [28]. We here conducted behavioral tests on this AD mouse model to examine memory deficits, while the ELISA, Thioflavins S staining of amyloid plaques, and other biochemical analyses provided pathological insight. In our studies, two time-point groups, pre-onset and post-onset stages, were used. The rationale for these time points stems from the fact that previous studies have shown little or no neuronal plaques at 5 months of age [26]. Thus, mice between 4 and 5 months of age represents the pre-onset stage of the disease. Over time, with the accelerated deposition of neuronal plaques after 9 months, it is expected that the quantity of neuronal plaques in the brain will be similar to that in a phenotypically observable AD patient and this represents the post-onset stage.

In the RAWM test, more behavioral differences were seen on day 2 after allowing the mice to rest for 24 h following day1 training and thus allowing us to test for long term memory.

At the pre-onset stage, we noticed no difference between the AD and AD/TG groups. We also noticed that two groups of mice did not show any spatial learning impairment at the end of the either day 1 or day 2. This is expected based on the fact that there would be very little deposition of amyloid plaques at this stage, which correlates with the lack of phenotypic difference and precedes any clinical presentation as seen in humans. At the post-onset stage, the AD/TG group made fewer errors compared to the AD group. This is in accordance with the fact that previous studies have shown that PSEN mutations increases the levels of Aβ peptides [36] while overexpression of Ubqln1 stabilizes PSEN1 proteins [15], which may lead to reduced levels of $A\beta_{40}$ and $A\beta_{42}$ and less memory impairment in the AD/TG mice as observed in our results. On the other hand, overexpression of Ubqln1 also decreases the levels of PEN-2 and nicastrin [37], two essential components of the γ-secretase complex, which may also lead to reduced AD phenotypes.

It was also evident that the post-onset AD group mice showed spatial learning and memory deficits by the end of day 1 and 2 respectively. This was unlike the post-onset AD/TG that showed improvement by the end of day 2. Additionally, it was shown that the post-onset AD mice made more errors and showed more spatial learning and memory deficits than its pre-onset AD counterpart, while there were no significant differences between the pre- and post-onset AD/TG groups, indicating that memory deficits worsen with age as the disease progresses.

The string test did not show any difference between the two genotypes at the pre-onset stage. However, the AD/TG group showed an increased motor agility and forepaw strength at the post-onset stage. Further comparisons did show worsening of motor agility and forepaw strength in the AD group with increasing age unlike the AD/TG group that showed no difference. This is in accordance with the possibility that motor functions are not impaired until the later stages of the disease which was observed only in the post-onset stage in our study. Further studies involving the rotarod test also showed a similar pattern as observed with the string test, with no difference seen between the two groups until the post-onset stages when the AD/TG group spent more time on the rotarod machine than the AD group. Additionally, there was worsening of the motor co-ordination in the AD group with increasing age in contrast to the AD/TG group that did not show any worsening with age. This indicates that the AD/TG group showed better motor function than the AD mice. This is also in accordance with the expected progression of AD in which motor function is not necessarily affected until the late stages of the disease. This was clearly exemplified in our study in the post-onset group.

Our ELISA experiments that specifically target $A\beta_{40}$ and $A\beta_{42}$ showed reduction in the amount of $A\beta_{40}$ and $A\beta_{42}$ in the cerebral cortex at both pre- and post-onset stages in the AD/TG group when compared to the AD group. Reduction of the peptides was also observed in the hippocampal region of AD/TG mouse brain. The hippocampal and cortical regions are usually affected with deposition of amyloid plaques consisting of toxic Aβ and show less toxic $A\beta_{40}$ and $A\beta_{42}$ proteins in the hippocampus at 5 months in this AD mouse model [38]. This could account for the behavioral differences observed between the AD and AD/TG groups at both ages. These ELISA data were consistent with the results of the amyloid plaques of cerebral cortex of the various groups. At the pre-onset stage, little or no

plaques were observed, which is in accordance with previous literature [19]. Reduced amyloid plaques were observed in the AD/TG group when compared to the AD group at pre- and post-onset stages. This was in accordance with our ELISA study in these age groups as reduction in $A\beta_{40}$ and $A\beta_{42}$ peptides would translate to reduction in the number of amyloid plaques.

Our observation showing that overexpression of Ubqln1 reduced mature AβPP protein level in the hippocampus was in accordance with the previous data indicating that downregulation of Ubqln1 increased mature AβPP [19]. Reduced mature AβPP level might lead to decreased Aβ production. As we did not observe significant alterations of C83, C99 and AβPP intracellular domain (AICD) (unpublished observations) in the AD/TG mouse brain when compared to those in AD mouse brain, overexpression of Ubqln1 may not affect AβPP processing in the AD mouse brains. This is different from a previous report showing that overexpression of Ubqln1 increased AICD level in SH-SY5Y cells [17]. Intriguingly, in another report, it was observed that downregulation of Ubqln1 did not affect AICD level in a different cell line [19]. These inconsistent observations may be caused by different cells utilized in the experiments.

Unlike those small ubiquitin-like proteins, such as SUMO [7] and NEDD8 [8–10], Ubqln1 cannot be covalently conjugated to target proteins in order to regulate targeted protein degradation. Instead, Ubqln1 is considered to function as a ubiquitin/polyubiquitin receptor and as an adapter linking ubiquitinated proteins to protein degradation machineries, i.e. UPS [11, 35] and/or autophagy pathways [13, 39]. Our results showed that overexpression of Ubqln1 did not affect ubiquitinated APP level in AD/TG mice when compared to that in AD mice. Thus, the decreased level of mature APP may not be caused by altered APP ubiquitination level through Ubqln1. It is possible that overexpression of Ubqln1 affects the endolysosomal pathway, leading to reduced APP maturation.

In summary, our data support that overexpression of Ubqln1 improves mouse spatial learning and memory and alleviates memory and learning deficits in AD mice. We also showed the biochemical and pathological basis for the alleviated symptoms observed. These results provide a strong rationale for us to explore new treatment options involving the Ubqln1-mediated intracellular molecular mechanisms that would alleviate neurological deficits associated with amyloid deposition.

Acknowledgments

We would like to thank the donors of the Alzheimer’s disease Research, a program of the BrightFocus Foundation, the Center for Brain and Behavior Research at the University of South Dakota, the South Dakota Board of Regents, and NIH (NS084340 & NS088084) for support of this research. We would also like to thank Dr. Scot Ouellette at the University of South Dakota (USD) for help in fluorescence microscopy, Dr. Doug Martin at USD for his assistance in navigating the data analysis, and Dr. David Diamond at the University of South Florida for technical assistance in the RAWM test.

References

1. Alzheimer's Association. 2015 Alzheimer's disease facts and figures. Alzheimers Dement. 2015; 11:332–384. [PubMed: 25984581]

2. Zhu X, Lee HG, Perry G, Smith MA. Alzheimer disease, the two-hit hypothesis: an update. Biochim Biophys Acta. 2007; 1772:494–502. [PubMed: 17142016]
3. Vetrivel KS, Thinakaran G. Amyloidogenic processing of β-amyloid precursor protein in intracellular compartments. Neurology. 2006; 66:S69–S73.
4. Yamada K, Toshitaka N. Therapeutic approaches to the treatment of Alzheimer's disease. Drugs Today (Barc). 2002; 38:631–637. [PubMed: 12582450]
5. Francis R, McGrath G, Zhang J, Ruddy DA, Sym M, Apfeld J, Nicoll M, Maxwell M, Hai B, Ellis MC. aph-1 and pen-2 are required for Notch pathway signaling, γ-secretase cleavage of βAPP, and presenilin protein accumulation. Developmental cell. 2002; 3:85–97. [PubMed: 12110170]
6. Jankowsky JL, Fadale DJ, Anderson J, Xu GM, Gonzales V, Jenkins NA, Copeland NG, Lee MK, Younkin LH, Wagner SL. Mutant presenilins specifically elevate the levels of the 42 residue β-amyloid peptide in vivo: evidence for augmentation of a 42-specific γ secretase. Human molecular genetics. 2004; 13:159–170. [PubMed: 14645205]
7. Lee L, Sakurai M, Matsuzaki S, Arancio O, Fraser P. SUMO and Alzheimer's disease. Neuromolecular Med. 2013; 15:720–736. [PubMed: 23979993]
8. Chen Y, Bodles AM, McPhie DL, Neve RL, Mrak RE, Griffin WS. APP-BP1 inhibits Abeta42 levels by interacting with Presenilin-1. Mol Neurodegener. 2007; 2:3. [PubMed: 17286867]
9. Chen Y, Neve R, Zheng H, Griffin W, Barger S, Mrak R. Cycle on Wheels: Is APP Key to the AppBp1 Pathway? Austin Alzheimers Parkinsons Dis. 2014; 1(2):pii:id1008.
10. Chen Y, Neve RL, Liu H. Neddylation dysfunction in Alzheimer's disease. J Cell Mol Med. 2012; 16:2583–2591. [PubMed: 22805479]
11. Ko HS, Uehara T, Tsuruma K, Nomura Y. Ubiquilin interacts with ubiquitylated proteins and proteasome through its ubiquitin-associated and ubiquitin-like domains. FEBS Lett. 2004; 566:110–114. [PubMed: 15147878]
12. Kleijnen MF, Shih AH, Zhou P, Kumar S, Soccio RE, Kedersha NL, Gill G, Howley PM. The hPLIC proteins may provide a link between the ubiquitination machinery and the proteasome. Mol Cell. 2000; 6:409–419. [PubMed: 10983987]
13. Rothenberg C, Srinivasan D, Mah L, Kaushik S, Peterhoff CM, Ugolino J, Fang S, Cuervo AM, Nixon RA, Monteiro MJ. Ubiquilin functions in autophagy and is degraded by chaperone-mediated autophagy. Hum Mol Genet. 2010; 19:3219–3232. [PubMed: 20529957]
14. Liu Y, Lu L, Hettinger CL, Dong G, Zhang D, Rezvani K, Wang X, Wang H. Ubiquilin-1 protects cells from oxidative stress and ischemic stroke caused tissue injury in mice. J Neurosci. 2014; 34:2813–2821. [PubMed: 24553923]
15. Mah AL, Perry G, Smith MA, Monteiro MJ. Identification of ubiquilin, a novel presenilin interactor that increases presenilin protein accumulation. J Cell Biol. 2000; 151:847–862. [PubMed: 11076969]
16. Viswanathan J, Haapasalo A, Bottcher C, Miettinen R, Kurkinen KM, Lu A, Thomas A, Maynard CJ, Romano D, Hyman BT, Berezovska O, Bertram L, Soininen H, Dantuma NP, Tanzi RE, Hiltunen M. Alzheimer's disease-associated ubiquilin-1 regulates presenilin-1 accumulation and aggresome formation. Traffic. 2011; 12:330–348. [PubMed: 21143716]
17. Viswanathan J, Haapasalo A, Kurkinen KM, Natunen T, Makinen P, Bertram L, Soininen H, Tanzi RE, Hiltunen M. Ubiquilin-1 modulates gamma-secretase-mediated epsilon-site cleavage in neuronal cells. Biochemistry. 2013; 52:3899–3912. [PubMed: 23663107]
18. El Ayadi A, Stieren ES, Barral JM, Boehning D. Ubiquilin-1 regulates amyloid precursor protein maturation and degradation by stimulating K63-linked polyubiquitination of lysine 688. Proc Natl Acad Sci U S A. 2012; 109:13416–13421. [PubMed: 22847417]
19. Hiltunen M, Lu A, Thomas AV, Romano DM, Kim M, Jones PB, Xie Z, Kounnas MZ, Wagner SL, Berezovska O, Hyman BT, Tesco G, Bertram L, Tanzi RE. Ubiquilin 1 modulates amyloid precursor protein trafficking and Abeta secretion. J Biol Chem. 2006; 281:32240–32253. [PubMed: 16945923]
20. Mizukami K, Abrahamson EE, Mi Z, Ishikawa M, Watanabe K, Kinoshita S, Asada T, Ikonomovic MD. Immunohistochemical analysis of ubiquilin-1 in the human hippocampus: association with neurofibrillary tangle pathology. Neuropathology. 2014; 34:11–18. [PubMed: 23869942]

21. Stieren ES, El Ayadi A, Xiao Y, Siller E, Landsverk ML, Oberhauser AF, Barral JM, Boehning D. Ubiquilin-1 is a molecular chaperone for the amyloid precursor protein. J Biol Chem. 2011; 286:35689–35698. [PubMed: 21852239]
22. Natunen T, Takalo M, Kemppainen S, Leskela S, Marttinen M, Kurkinen KM, Pursiheimo JP, Sarajarvi T, Viswanathan J, Gabbouj S, Solje E, Tahvanainen E, Pirttimaki T, Kurki M, Paananen J, Rauramaa T, Miettinen P, Makinen P, Leinonen V, Soininen H, Airenne K, Tanzi RE, Tanila H, Haapasalo A, Hiltunen M. Relationship between ubiquilin-1 and BACE1 in human Alzheimer's disease and APdE9 transgenic mouse brain and cell-based models. Neurobiol Dis. 2016; 85:187–205. [PubMed: 26563932]
23. Bertram L, Hiltunen M, Parkinson M, Ingelsson M, Lange C, Ramasamy K, Mullin K, Menon R, Sampson AJ, Hsiao MY, Elliott KJ, Velicelebi G, Moscarillo T, Hyman BT, Wagner SL, Becker KD, Blacker D, Tanzi RE. Family-based association between Alzheimer's disease and variants in UBQLN1. N Engl J Med. 2005; 352:884–894. [PubMed: 15745979]
24. Zhang T, Jia Y. Meta-analysis of Ubiquilin1 gene polymorphism and Alzheimer's disease risk. Med Sci Monit. 2014; 20:2250–2255. [PubMed: 25387430]
25. Yue Z, Wang S, Yan W, Zhu F. Association of UBQ-8i polymorphism with Alzheimer's disease in Caucasians: a meta-analysis. Int J Neurosci. 2015; 125:395–401. [PubMed: 25010605]
26. Jankowsky JL, Fadale DJ, Anderson J, Xu GM, Gonzales V, Jenkins NA, Copeland NG, Lee MK, Younkin LH, Wagner SL, Younkin SG, Borchelt DR. Mutant presenilins specifically elevate the levels of the 42 residue beta-amyloid peptide in vivo: evidence for augmentation of a 42-specific gamma secretase. Hum Mol Genet. 2004; 13:159–170. [PubMed: 14645205]
27. King DL, Arendash GW, Crawford F, Sterk T, Menendez J, Mullan MJ. Progressive and gender-dependent cognitive impairment in the APP(SW) transgenic mouse model for Alzheimer's disease. Behav Brain Res. 1999; 103:145–162. [PubMed: 10513583]
28. Alamed J, Wilcock DM, Diamond DM, Gordon MN, Morgan D. Two-day radial-arm water maze learning and memory task; robust resolution of amyloid-related memory deficits in transgenic mice. Nat Protoc. 2006; 1:1671–1679. [PubMed: 17487150]
29. Park CR, Zoladz PR, Conrad CD, Fleshner M, Diamond DM. Acute predator stress impairs the consolidation and retrieval of hippocampus-dependent memory in male and female rats. Learn Mem. 2008; 15:271–280. [PubMed: 18391188]
30. Arendash GW, King DL, Gordon MN, Morgan D, Hatcher JM, Hope CE, Diamond DM. Progressive, age-related behavioral impairments in transgenic mice carrying both mutant amyloid precursor protein and presenilin-1 transgenes. Brain Res. 2001; 891:42–53. [PubMed: 11164808]
31. Arendash GW, King DL, Gordon MN, Morgan D, Hatcher JM, Hope CE, Diamond DM. Progressive, age-related behavioral impairments in transgenic mice carrying both mutant amyloid precursor protein and presenilin-1 transgenes. Brain research. 2001; 891:42–53. [PubMed: 11164808]
32. Ly PT, Cai F, Song W. Detection of neuritic plaques in Alzheimer's disease mouse model. J Vis Exp. 2011
33. Liu Y, Hettinger CL, Zhang D, Rezvani K, Wang X, Wang H. The proteasome function reporter GFPu accumulates in young brains of the APPswe/PS1dE9 Alzheimer's disease mouse model. Cell Mol Neurobiol. 2014; 34:315–322. [PubMed: 24363091]
34. Diamond DM, Park CR, Heman KL, Rose GM. Exposing rats to a predator impairs spatial working memory in the radial arm water maze. Hippocampus. 1999; 9:542–552. [PubMed: 10560925]
35. Wang H, Monteiro MJ. Ubiquilin interacts and enhances the degradation of expanded-polyglutamine proteins. Biochem Biophys Res Commun. 2007; 360:423–427. [PubMed: 17603015]
36. Petanceska SS, Seeger M, Checler F, Gandy S. Mutant presenilin 1 increases the levels of Alzheimer amyloid beta-peptide Abeta42 in late compartments of the constitutive secretory pathway. J Neurochem. 2000; 74:1878–1884. [PubMed: 10800930]
37. Massey LK, Mah AL, Monteiro MJ. Ubiquilin regulates presenilin endoproteolysis and modulates gamma-secretase components, Pen-2 and nicastrin. Biochem J. 2005; 391:513–525. [PubMed: 15975090]

38. Kelley CM, Perez SE, Overk CR, Wynick D, Mufson EJ. Effect of neocortical and hippocampal amyloid deposition upon galaninergic and cholinergic neurites in AbetaPPswe/PS1DeltaE9 mice. J Alzheimers Dis. 2011; 25:491–504. [PubMed: 21471639]

39. N'Diaye EN, Kajihara KK, Hsieh I, Morisaki H, Debnath J, Brown EJ. PLIC proteins or ubiquilins regulate autophagy-dependent cell survival during nutrient starvation. EMBO Rep. 2009; 10:173–179. [PubMed: 19148225]

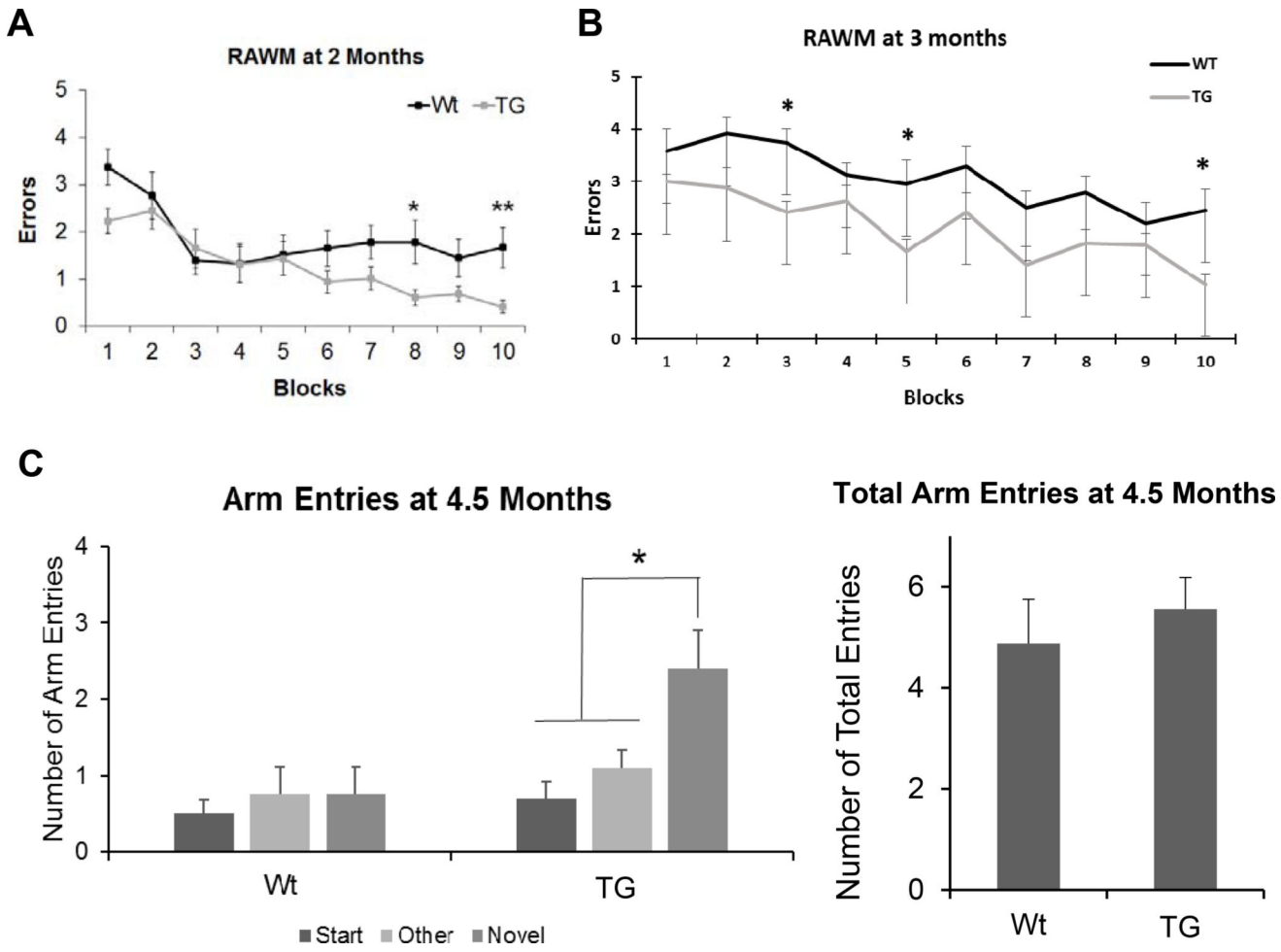

Figure 1. Overexpression of Ubqln1 improves spatial learning and memory in mice

(A) Measurement of mouse spatial learning and memory at 2 months in Wt and TG mice by RAWM test. N = 17 per group. **(B)** Measurement of mouse spatial learning and memory using a different cohort of Wt and TG mice at 3 months by RAWM test. N = 10 per group. **(C)** Measurement of mouse spatial learning and memory using another different cohort of Wt and TG mice at 4.5 months by Y-maze test. The number for each arm entries are shown on the left panel and the total number of arm entries are shown on the right panel. Wt, n = 8; TG, n = 9. Data are shown as mean ± SEM. *p < 0.05, ** p < 0.01.

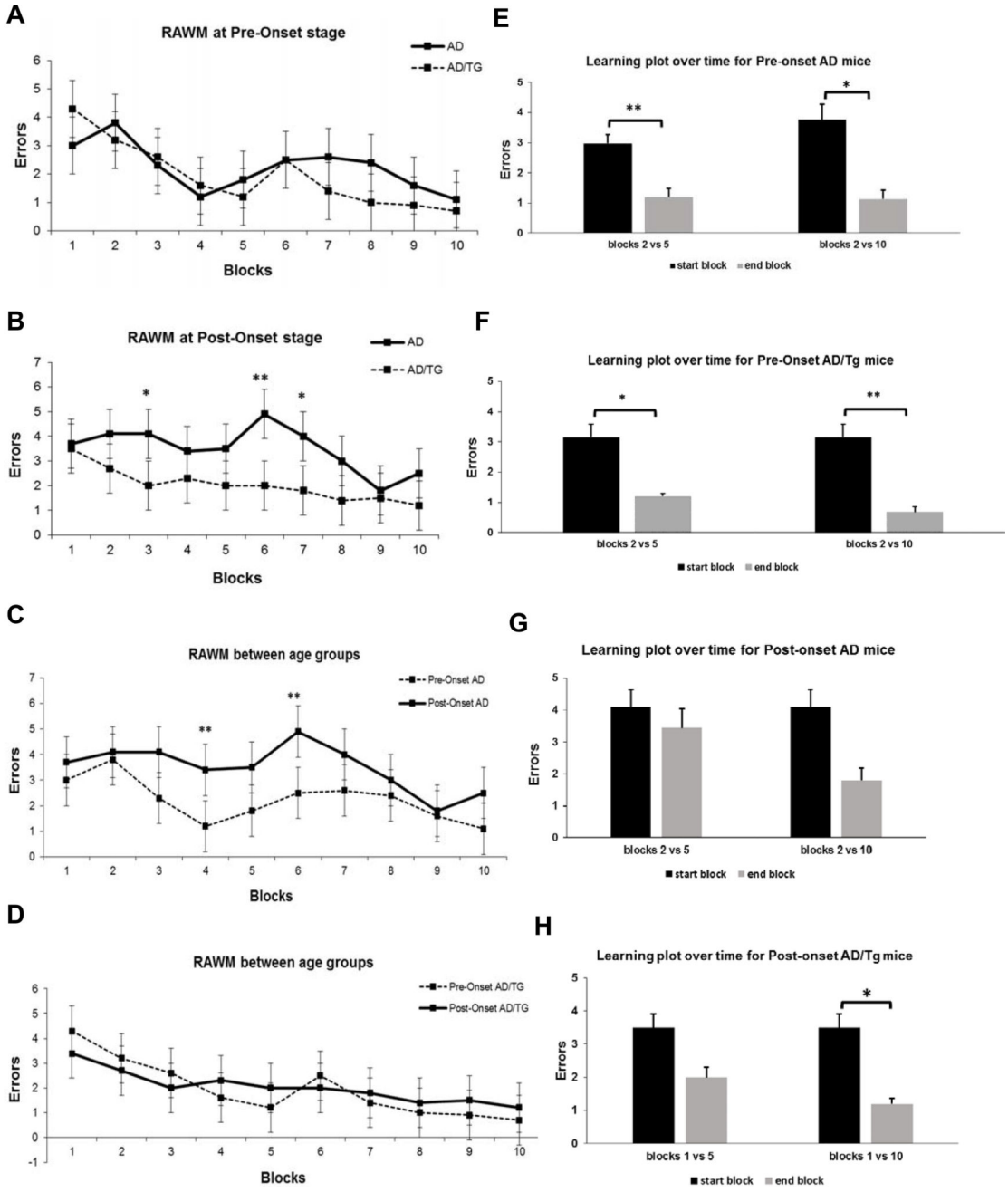

Figure 2. AD/TG mice show better spatial learning and memory than age-matched AD mice

(A), (B) Measurement of mouse spatial learning and memory between the two genotypes at pre-onset **(A)**, and post-onset **(B)**. **(C), (D)** Measurement of mouse spatial learning and memory between different ages in genotype-matched mice in AD mice **(C)** and AD/TG mice **(D)**. **(E), (F), (G), (H)** Measurement of mouse spatial learning and memory over blocks of trials in pre-onset AD **(E)**, pre-onset AD/TG mice **(F)**, post-onset AD **(G)**, and post-onset AD/TG **(H)** by RAWM test. Data are shown as mean ± SEM. N = 8 per group. *p < 0.05, ** p < 0.01.

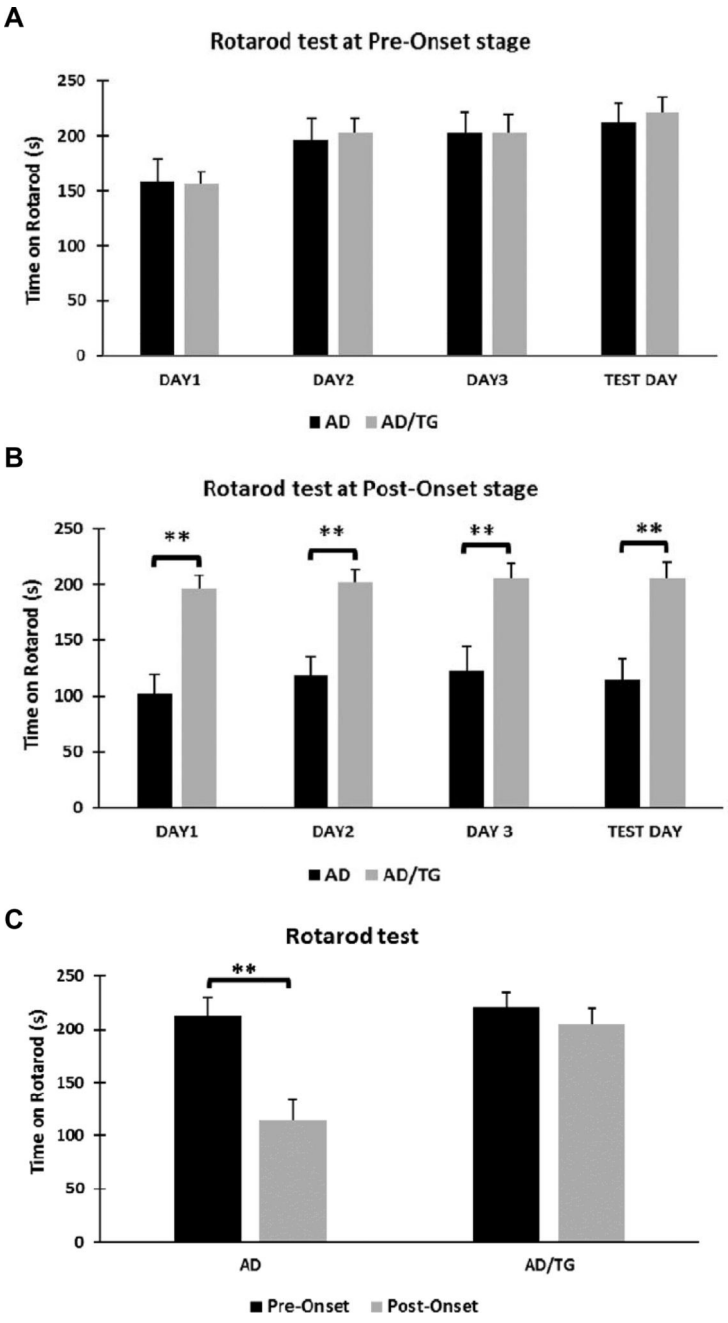

Figure 3. AD/TG mice exhibit improved motor function and co-ordination compared to age-matched AD mice

(A), (B) Measurement of motor function and co-ordination between the two genotype mice at pre-onset stage **(A)** and post-onset stage **(B)**. **(C)** Comparison of motor function and co-ordination between the two age groups in each genotype mice by rotarod test. N = 10 per group. Data are shown as mean ± SEM. ** $p < 0.01$.

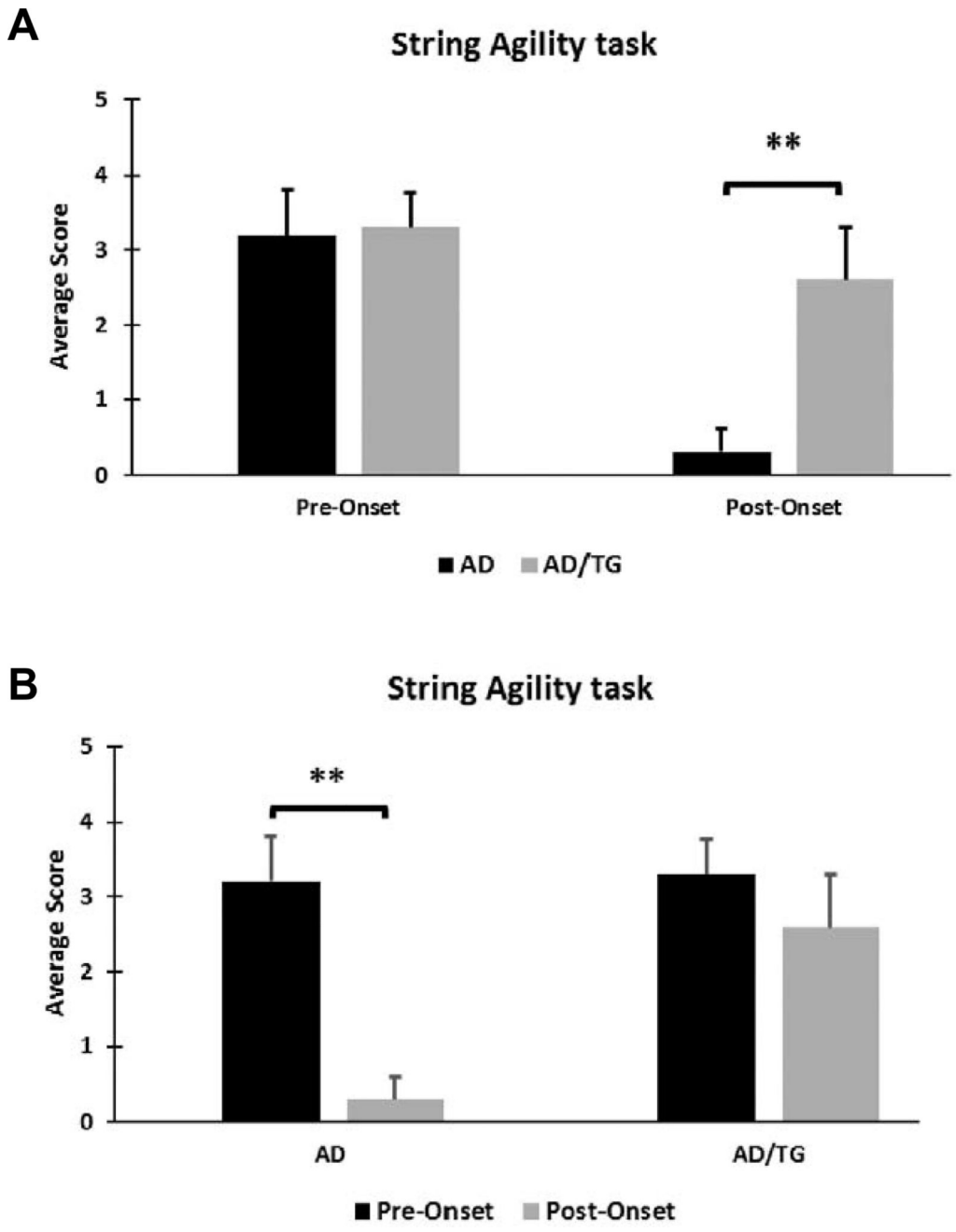

Figure 4. AD/TG mice exhibit improved agility and forepaw strength compared to age-matched AD mice

(A) Measurement of forepaw grip ability and agility in AD and AD/TG mice at pre- and post-onset stages. **(B)** Measurement of forepaw grip ability and agility with age in each genotype by string agility test. N = 10 per group. Data are shown as mean ± SEM. ** $p < 0.01$.

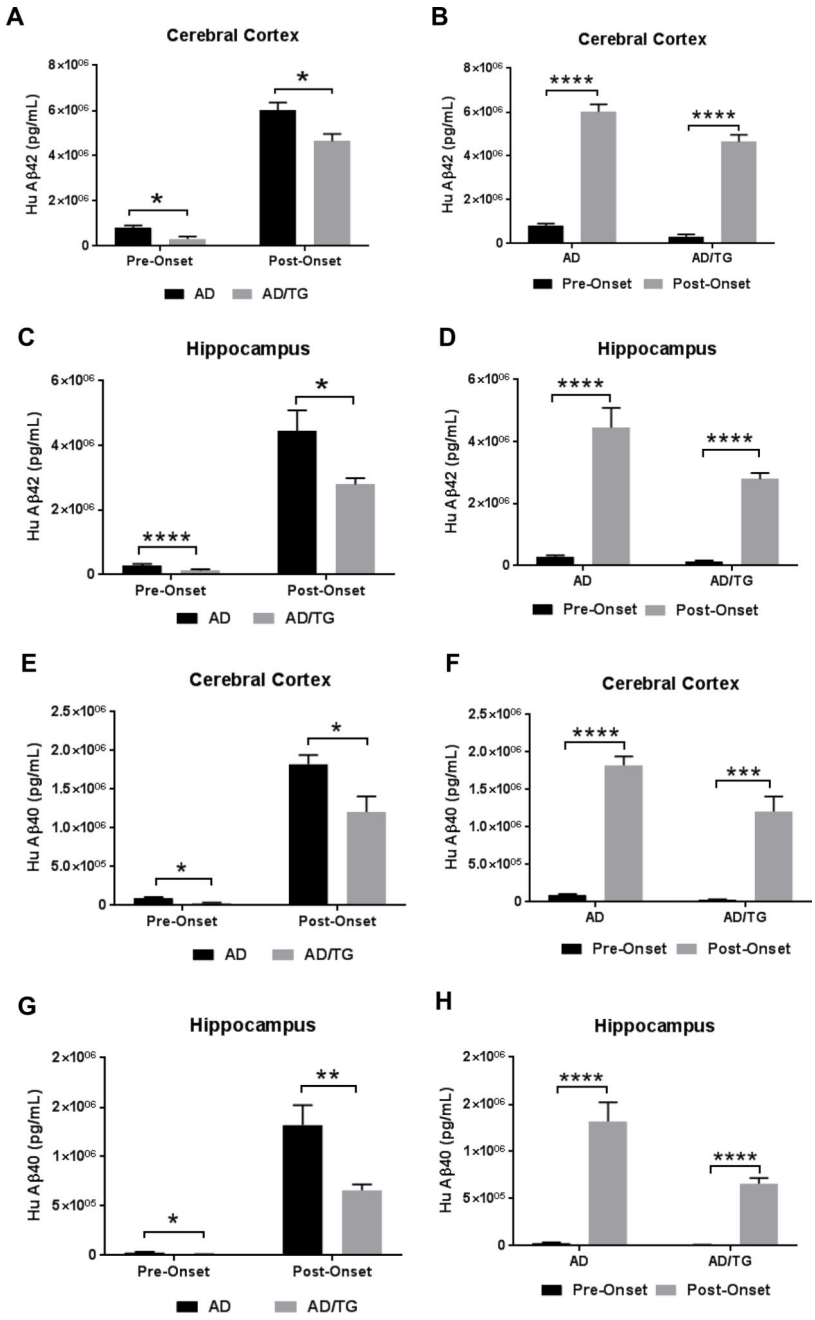

Figure 5. Significant reduction of human Aβ_{42} and Aβ_{40} levels in the cerebral cortex and hippocampus of AD/TG mice compared to age-matched AD mice

(A) Measurement of human Aβ_{42} level in the cerebral cortex of AD and AD/TG mice at pre- and post-onset stages by ELISA. **(B)** Measurement of human Aβ_{42} level in the cerebral cortex with age in each genotype by ELISA. Pre-Onset: AD, n = 9; AD/TG, n = 5; Post-Onset: AD, n = 5; AD/TG, n = 6. **(C)** Measurement of human Aβ_{42} level in the hippocampus of AD and AD/TG mice at pre- and post-onset stages. **(D)** Measurement of human Aβ_{42} level in the hippocampus with age in each genotype by ELISA. Pre-onset: AD, n = 10; AD/TG, n = 6; Post-onset: AD, n = 6; AD/TG, n = 6. **(E)** Measurement of human

$A\beta_{40}$ level in the cerebral cortex of AD and AD/TG mice at pre- and post-onset stages by ELISA. **(F)** Measurement of human $A\beta_{40}$ level in the cerebral cortex with age in each genotype by ELISA. Pre-onset: AD, n = 9; AD/TG, n = 5; Post-onset: AD, n = 5; AD/TG, n = 5. **(G)** Measurement of human $A\beta_{40}$ level in the hippocampus of AD and AD/TG mice at pre- and post-onset stages. **(H)** Measurement of human $A\beta_{40}$ level in the hippocampus with age in each genotype by ELISA. Pre-onset: AD, n = 9; AD/TG, n = 5; Post-onset: AD, n = 5; AD/TG, n = 6. Data are shown as mean ± SEM. *p < 0.05, ***p < 0.001, ****p < 0.0001.

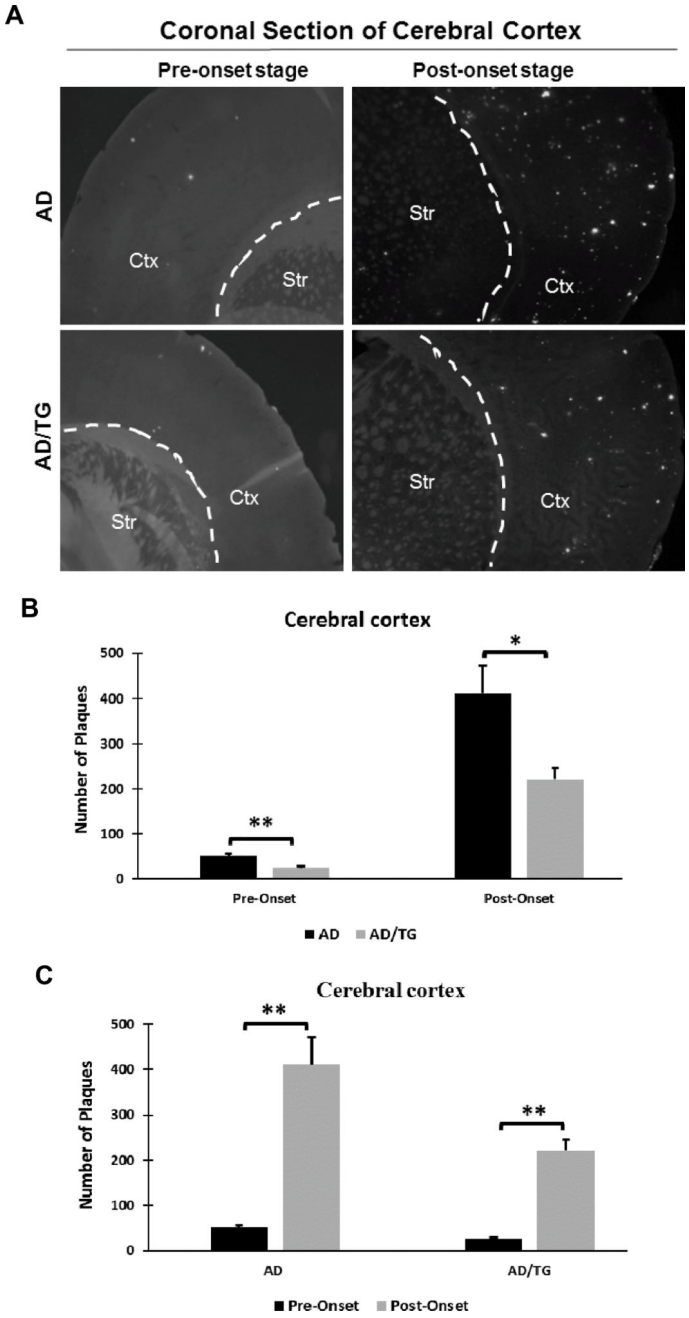

Figure 6. The amyloid plaque number is significantly decreased in the cerebral cortex of AD/TG mice compared to age-matched AD mice over time

(A) Representative images of Thioflavin S staining in cerebral cortex of AD and AD/TG mice at pre- and post-onset stages. **(B)** Quantification of Aβ plaques in the cerebral cortex of AD and AD/TG mice at pre- and post-onset stages. **(C)** Quantification Aβ plaques in the cerebral cortex with age in each genotype. For pre-onset stage: AD, n = 8; AD/TG, n = 5. For post-onset stage: AD, n = 4; AD/TG, n = 6. Numerical data are shown as mean ± SEM. *$p < 0.05$, ** $p < 0.01$.

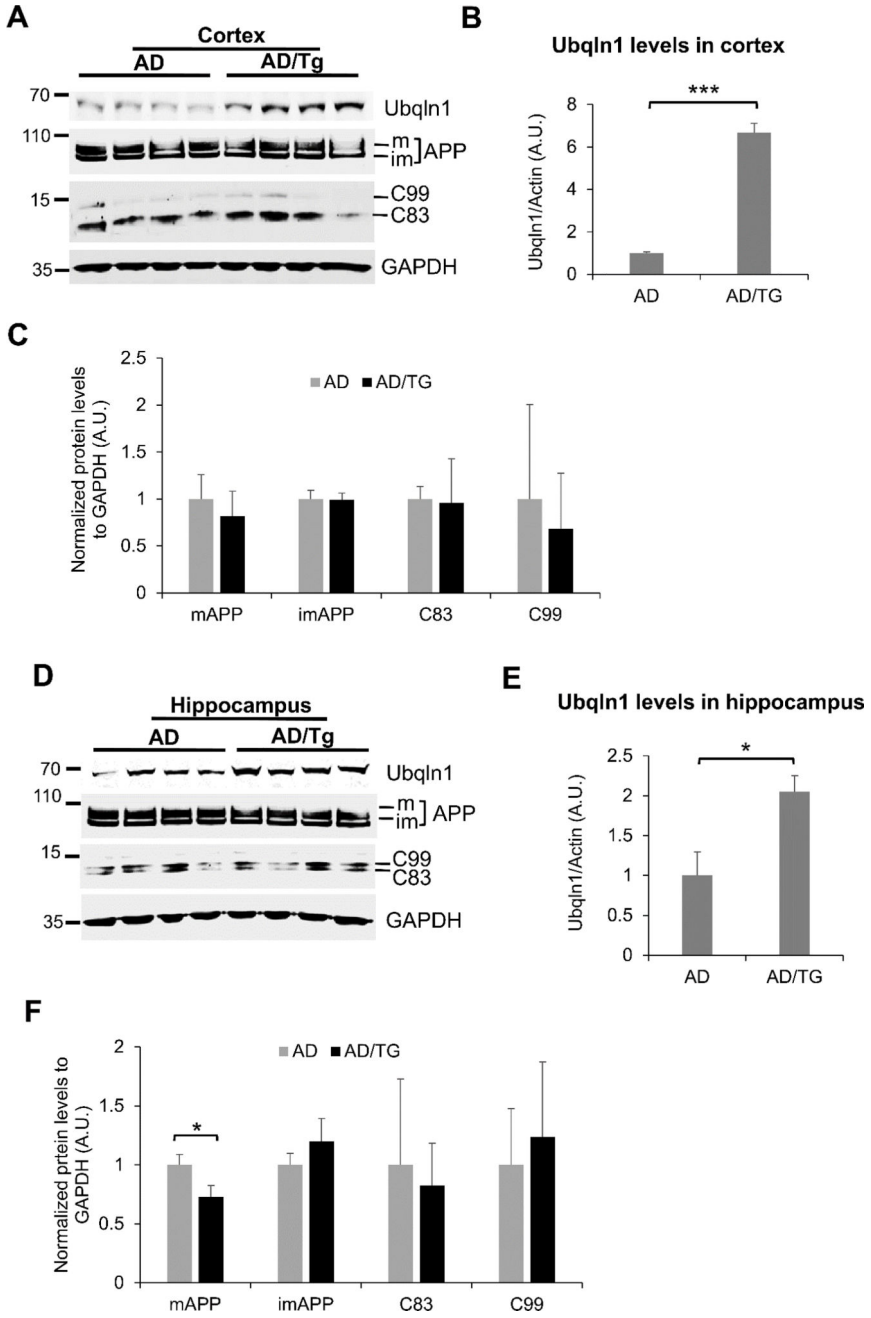

Figure 7. Overexpression of Ubqln1 reduces AβPP maturation in the hippocampus of post-onset AD mice

Western blot analysis of Ubqln1, AβPP, and C99 and C83 fragment levels in the cortex **(A)** and hippocampus **(D)**. Quantification of Ubqln1 protein expression level in post-onset stage cerebral cortex **(B)** and hippocampus **(E)**. Quantification of immature and mature AβPP as well as C99 and C83 fragment levels in the cortex **(C)** and hippocampus **(F)**. Numerical data are shown as mean ± SD. *$p < 0.05$; ***$p < 0.0001$; $n = 4$ for both AD and AD/TG groups.

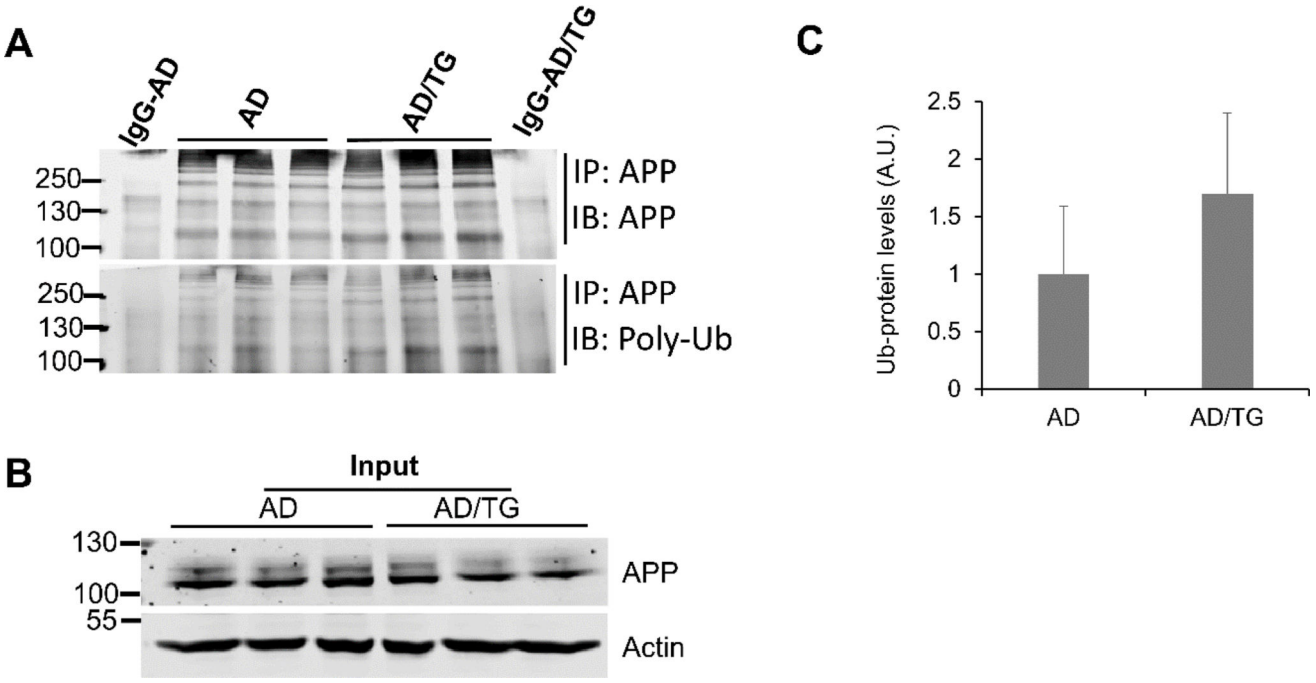

Figure 8. Overexpression of Ubqln1 does not affect AβPP ubiquitination in post-onset AD cortex

(A) AβPP in the cortex was immunoprecipitated (IP) with a C-terminal antibody and then immunoprobed either with an anti-AβPP (upper panel) or with an anti-ubiquitin antibody (lower panel). **(B)** AβPP level in the input. Immunoblotting of actin was used as a loading control. **(C)** Quantitation of ubiquitinated AβPP levels in AD and AD/TG cortex. Numerical data are shown as mean ± SD. $p > 0.05$; $n = 3$ for both AD and AD/TG groups.